Dictyostelium Myosin II G680V Suppressors Exhibit Overlapping Spectra of Biochemical Phenotypes Including Facilitated Phosphate Release

Yuan Wu,[1] Mike Nejad[2] and Bruce Patterson

Department of Molecular and Cell Biology, University of Arizona, Tucson, Arizona 85721

Manuscript received December 22, 1998
Accepted for publication May 17, 1999

ABSTRACT

We have biochemically characterized 13 intragenic suppressors of the G680V mutation of Dictyostelium myosin II. In the absence of the G680V mutation, the suppressors result in a number of deviant behaviors, most commonly an increase in the basal (actin-independent) ATPase of the motor. This phenotype is complementary to that of the G680V mutant and supports our proposal that the latter impairs phosphate release. Different subsets of the mutants also suffer from poor ATPase enhancement by 1 mg/ml actin, failure to release from actin in the presence of ATPγS (or ADP and salt), and excessive release from actin in the presence of ADP. The patterns of suppressor behaviors suggest that, in general, they are facilitating P_i-releasing state(s) of the motor, but that different individual suppressors may secondarily perturb other states or actions of the motor.

WHILE the myosin motor plays a diverse set of essential roles in eukaryotic cells, our understanding of the molecule as a mechanical device is still primitive. The inadequacy of our knowledge stems in large part from the tremendous difficulties involved in mapping out the different conformational states of the motor as it progresses through its cycle of actin attachment, movement, and release. The solution of a series of crystal structures of Dictyostelium myosin subfragments, albeit in actin-free forms, has provided a critical tool for deduction of the key states of the myosin cycle and their transitions. We are linking this information about the basic architecture of the motor to a series of genetic and biochemical "maps" with the goal of illuminating and perhaps "capturing" heretofore inaccessible states of the motor.

The G680V mutation of Dictyostelium myosin confers a number of highly suggestive properties on the motor (Patterson *et al.* 1997). G680V mutant myosin acts as a strong brake on wild-type motors in mixing experiments, which suggests an impairment during a strongly bound state. Genetically truncated (*i.e.*, non-filament-forming) G680V motors display an extended state that occurs during the ATPase cycle and exhibits salt-sensitive actin binding that matches neither the nucleotide-free, ATPγS-bound nor ADP-bound states of wild-type or G680V motors. These findings have led us to hypothesize that the motor "hangs up" at the initiation of its working stroke because of an impairment of its inorganic phosphate (P_i) release.

To test this prediction and to learn more about this unique mutant, we have isolated and genetically characterized more than a score of intragenic suppressors of the G680V mutation (Patterson 1998). The suppressors show striking clustering within the three-dimensional structure, and many render the motor biologically defunct in the absence of the G680V change. Knowing where the suppressors are situated, however, allows only variably informed guesses as to how they are acting. For this reason, we have embarked on a biochemical survey of the gross properties of the suppressors. Our results indicate that in the family of suppressors that shows the tightest spatial clustering, all suppressors share the property of accelerating the motor's basal ATPase. This phenotype is satisfying in that it is appropriate for suppressors of a mutant defective in P_i release, and that it allows us to propose a specific mechanical model for the action of the G680V mutation and the majority of its suppressors. Our results also reveal a constellation of alterations in some of the suppressors' actin interaction properties induced by different nucleotides.

MATERIALS AND METHODS

Strains and media: The nonaggregating SPERA cell line (Patterson 1998) was used for all experiments. Cell culture conditions were as described by Sussman (1987).

Plasmids and transformation: All plasmids expressing truncated (S1) forms of myosin were derived from pTIKL · S1-His (Giese and Spudich 1997) by using convenient restriction sites to replace the appropriate region of the myosin heavy chain gene with a fragment containing single or double muta-

Corresponding author: Bruce Patterson, LSS525, Department of Molecular and Cell Biology, University of AZ, Tucson, Arizona 85721. E-mail: patterso@u.arizona.edu

[1] *Current address:* Bioprocess Research and Development, Eli Lilly & Co., Lilly Corporate Ctr., Indianapolis, IN 46285.

[2] *Current address:* Oregon Health Sciences University, School of Medicine, Portland, OR 97201-3098.

tions. Truncated myosins produced from these plasmids are referred to in the text as S1.X###X, *e.g.*, S1.G680V, to distinguish them from full-length myosins. Plasmids expressing full-length myosins have been reported previously (Patterson 1998). Plasmids were introduced via electroporation using the following protocol: cells were harvested from confluent, 100-mm Petri dishes after thorough aspiration of all media. Cells were harvested using gentle trituration with 1.5-ml ice-cold E-pore buffer (50 mm sucrose and 10 mm $NaPO_4$) and spun gently in an Eppendorf tube for 30 sec. Cells were resuspended in 300 μl E-pore buffer. Aliquots of 45 μl each were added to 1–2 ml of 0.2–2 mg/ml DNA (in 2 mm Tris 8.0 and 0.2 mm EDTA) and transferred to an ice-cold, 0.1-cm electroporation cuvette. Electroporation conditions were 400 or 800 V, 3 μF and 1000 Ω resistance. After electroporation, 350 μl of cold HL-5 supplemented with heat-killed *Klebsiella aerogenes* was added to the cuvettes. The mixture was then added to chilled six-well Petri dishes containing 1.5 ml HL-5. Cultures were incubated at 22° for 24 hr, and then G418 was added to bring cultures to 10 μg/ml G418. After an additional 24 hr, the media were replaced with HL-5 containing 8 μg/ml G418. Resulting transformants were combined for all further experiments. All sequencing was performed on pBluescript or pBC plasmids (Stratagene, La Jolla, CA) bearing PCR-derived fragments of the myosin gene, which were cloned using convenient restriction sites.

Chemicals: ATP (disodium salt, ~99% pure according to the manufacturer) was purchased from Sigma (St. Louis). ATPγS (tetralithium salt, >85% pure according to the manufacturer) was purchased from Calbiochem (San Diego, CA). All other reagents were from Sigma unless otherwise stated. Alkaline phosphatase was purchased from Boehringer Mannheim (Indianapolis, IN).

Preparation of myosin S1 and G-actin: Dictyostelium myosin S1 was prepared according to the method of Manstein and Hunt (1995) with modifications. Approximately 100 million cells from a confluent plate were washed in 15 ml ice-cold Bonner's solution (10 mm NaCl, 10 mm KCl, and 2 mm $CaCl_2$) and then treated in 20 mm NaN_3 for 10 min in Bonner's solution. Cells were washed with 1 ml wash buffer (50 mm Tris-HCl, pH 8.0 at 4°, 2.5 mm EGTA, 2 mm EDTA, 5 mm benzamidine and 2 mm 2-mercaptoethanol) containing 0.04% NaN_3 and were resuspended in 300 μl wash buffer containing 5 units of alkaline phosphatase and protease inhibitor mixes I and II. Protease inhibitor mix I (100×) contained 200 mm *N*-carboberzoxy-Pro-Ala, 10 mg/ml *N*-α-*p*-tosyl-l-arginine methyl ester (TAME), 8 mg/ml *N*-α-tosyl-phenylalanyl chloromethylketone, 0.2 mg/ml pepstatin, and 1.5 mg/ml leupeptin. Protease inhibitor II (1000×) contained 150 mm phenylmethylsulfonylfluoride. Cells were then lysed by adding 300 μl wash buffer containing 2% Triton X-100 and protease inhibitor mixes I and II and were incubated on ice for 30 min. Cytoskeletons were spun down in an Eppendorf microcentrifuge at 14,000 × *g* for 30 min at 4° and washed once with 500 μl wash buffer plus (50 mm Tris-HCl, pH 8.0 at 4°, 5 mm benzamidine, and 2 mm 2-mercaptoethanol). Cytoskeletons were resuspended in 50 μl wash buffer plus and then mixed with 50 μl wash buffer plus containing 20 mm Mg^{2+}-ATP (pH adjusted to 7.5) and 0.4 m KCl. After incubating on ice for 10 min, the mixture was centrifuged at 125,000 × *g* in a tabletop ultracentrifuge (TL-100; Beckman, Fullerton, CA) at 4° for 30 min. The supernatant was mixed with 10 μl Qiagen Ni-NTA resin and incubated in a cold room under rotation for 1 hr. After incubation, the resin was washed once with 0.5 ml elution buffer (30 mm imidazole, pH 8.0 at 4°, 5 mm benzamidine, and 2 mm 2-mercaptoethanol) containing 10 mm Mg^{2+}-ATP and 0.2 m KCl and twice with 0.5 ml elution buffer. The Dictyostelium myosin S1 was eluted in 20 μl of 200 mm imidazole buffer (pH 7.5 at 4°, 5 mm benzamidine, and 2 mm 2-mercaptoethanol) for 15 min in a cold room under rotation. The elution was repeated once.

G-actin was prepared from an acetone powder of chicken breast muscle by the method of Spudich and Watt (1971) and frozen at −80° until the day of use. F-actin was prepared by the polymerization of G-actin by adding 0.2 m KCl, 3 mm $MgCl_2$, 0.2 mm ATP, and 8 μg/ml phalloidin. F-actin was pelleted at 125,000 × *g* and resuspended in 10 mm imidazole, pH 7.5 at 4°, 8 μg/ml phalloidin, 2 mm 2-mercaptoethanol, and 75 mm KCl.

Myosin ATPase assays: Myosin S1 basal-level, 1 mg/ml actin-enhanced Mg^{2+}-ATPase, and high-salt Ca^{2+}-ATPase assays were performed in 70 mm imidazole, pH 7.5 at 20°, 1 mm DTT, 1.5 mm ATP, and ~0.2 μm S1 in a total volume of 120 μl. F-actin was added to a final concentration of 1 mg/ml in the actin-enhanced ATPase assays. Ca^{2+}-ATPase assays were done in the presence of 5 mm $CaCl_2$ and 0.6 m KCl instead of 2 mm $MgCl_2$.

Reactions were performed at 20° for 0.5–1.5 hr under conditions of linearity with respect to time and enzyme concentration. Aliquots of 33 μl each were taken at different time points for quantification of P_i by the colorimetric method (White 1982) and were checked for linearity. The enzyme activity unit was nanomoles of P_i per nanomoles of S1 per minute at 20°. Repeat experiments gave values within 25% of those reported.

Ultracentrifuge actin-binding experiments: F-Actin (~2 μm), S1 (0.05–0.1 μm), nucleotides (none, 1 mm ATP, 5 mm ADP or 1 mm ATPγS), and KCl (0 or 250 mm) in a 200-μl total volume were mixed well and incubated at 20° for 10 min. Samples were then quickly transferred into tubes and immediately spun in a Beckman TL-100 tabletop ultracentrifuge at 130,000 × *g* for 30 min. The ATPase rates of the mutants under the conditions of the experiment were insufficient to deplete the ATP present. The supernatants were discarded. Pellets were resuspended in wash buffer plus and run on an SDS-PAGE gel. The myosin S1 bands were stained with Coomassie blue and scanned on a transmissive scanner. Quantification of relative S1 amount was done using NIH image software. All measurements were made relative to standards run on the same gel. All values are taken from representative experiments; all experiments have been performed on at least two independent occasions. Variation between individual data points was routinely within 10 percentage points and never more than 20.

Stopped-flow experiments on Dictyostelium cytoskeletons: Dictyostelium cytoskeletons were prepared according to the method of Kuczmarski *et al.* (1991) with modifications. The Dictyostelium cells were first starved in starvation buffer (25 mm MES, 1 mm $MgCl_2$, and 0.1 mm $CaCl_2$, pH 6.8 at 20°) for 2 hr at room temperature in a shaking water bath. All subsequent procedures were performed at 4°. Cells were then sedimented and washed in wash buffer (100 mm PIPES, 2.5 mm EGTA, 1 mm $MgCl_2$, 10 mm TAME, and 20 mm benzamidine, pH 7.2 at 4°) at a concentration of 100 million cells/15 ml buffer and resuspended in lysis buffer (wash buffer plus 0.5% Triton X-100 and 10 μg/ml leupeptin) at a concentration of 100 million cells/ml buffer. After incubating on ice for 30 min, the resulting cytoskeletons were sedimented at 3500 rpm for 4 min in an Eppendorf centrifuge. They were then washed once with a half volume of lysis buffer and once with an equal volume of wash buffer. The final cytoskeletons were then suspended in wash buffer at ~50 million cytoskeletons/ml buffer for stopped-flow assays.

Stopped-flow experiments were performed in a stopped-flow device (RX1000 Rapid Kinetics from Applied Photophysics) at 20° monitored by a Hewlett-Packard 8453 spectrophotometer. The contraction of the cytoskeletons was measured

as an increase in absorbance at 310 arbitrary units (AU). Integration time was set at 0.1 sec. The initial contraction rate (arbitrary units per second) was calculated from the first 3 sec of data from the reaction using the curve-fitting software provided with the spectrophotometer or from the first 10-sec data using line (linear) fit, depending on the apparent rate. The initial contraction rate and the amplitude were standardized against the OD (AU) of the starting solution of cytoskeletons (0.6–1.2 AU).

RESULTS

Traditionally, biochemical analysis of myosins has been performed on vast quantities of painstakingly purified material. Such an approach is not well suited to our goal of rapidly surveying an extensive set of properties for large numbers of single and double mutants. For this reason, we have modified a variety of existing protocols to provide tools for rapid and efficient gross characterization of mutant myosins. The results presented here allow us to identify the most deranged feature(s) of a given mutant as compared to the wild type. In all cases, several variants of a given assay can be performed on up to a half-dozen of individual myosin motors within a span of 2–3 days.

Our purification procedure is similar to that of Manstein and Hunt (1995) and entails the use of heptahistidine-terminated, genetically engineered Dictyostelium myosin S1 (amino acids 1–865) and pTIKL-S1-His (Giese and Spudich 1997). ATPase assays were performed under the following conditions: (1) in Mg^{2+}-ATP in the absence of actin (basal ATPase); (2) same as the previous condition, but also in the presence of 1 mg/ml F-actin; and (3) using 5 mm Ca^{2+} instead of Mg^{2+} under high-salt (600 mm KCl) conditions (Ca^{2+}-ATPase). Actin-binding and -release assays were performed as cosedimentation assays. The percentage of added S1 pelleted during ultracentrifugation with actin filaments was assessed in the absence of nucleotide; in the presence of 1 mm ATP, 5 mm ADP, or 1 mm ATPγS; and in the presence or absence of 250 mm KCl. Data have been represented as soluble (non-actin-bound) to clearly represent the role of the added nucleotide.

The ability of full-length mutant myosins to support cytoskeletal contraction was assessed using a modification of the procedure of Kuczmarski and co-workers (Kuczmarski *et al.* 1991; Aguado-Velasco and Kuczmarski 1993). The initial rate of contraction and the final extent of contraction achieved were measured for triton-treated "ghosts" of cells expressing a full-length myosin bearing the appropriate mutation. Stopped-flow addition of ATP induced cytoskeletal contraction, which was assessed as a change in light scattering, measured as absorbance at 310 nm.

Our characterization focused on a subset of the intragenic suppressors of the G680V mutation that we have

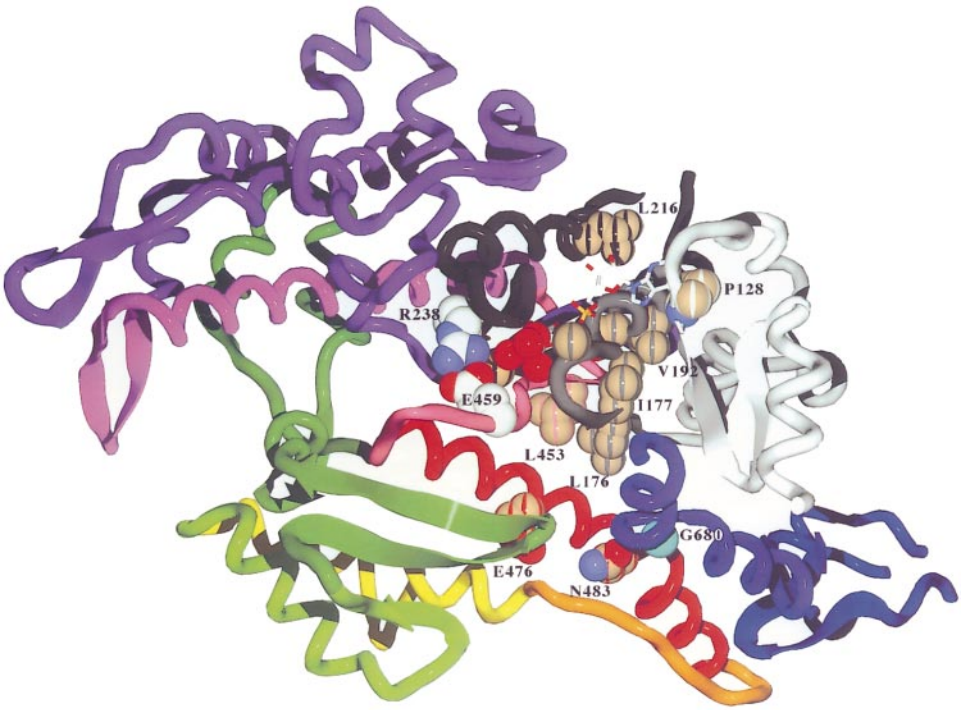

Figure 1.—Location of G680V and suppressors in the ADP·vanadate crystal structure of the Dictyostelium myosin II motor domain (Smith and Rayment 1996). Ribbon representation of residues 2–747 is shown. The region between amino acids 631 and 668 is omitted to avoid obscuring key features. Route of the polypeptide chain through the structure is indicated by color; the N terminus is off-white, progressing to black, followed by purple progressing through the spectrum to deep blue. Key regions are white (amino acids 1–140), dark gray (175–195), black (196–245), coral (442–465), red (466–496), and blue (669–691). G680 is in cyan. Suppressor positions are space filled, with carbons indicated in tan and stripes indicating the region of the polypeptide chain from which they arise (*e.g.*, L216 is tan with black stripes since it lies in the 196–245 sequence). Residues are numbered where space permits. ADP is shown as a stick model, vanadate is space filled in red, and the R238-E459 salt bridge is space filled using CPK coloring.

TABLE 1

Comparison of mutant and wild-type motor properties

Mutant	ATPase[a]			Contraction[b]	
	%WT basal	1 mg/ml actin (%WT)/↑/%WT ↑	%Ca^{2+}/salt	Rate[c]	Extent[d]
Wild type	100	(100)/5.8×/100	100	100	100
G680V	10	(20)/9.5×/170	3	2	60
P128Q	70	(115)/10×/180	30	0	0
L175F	150	(90)/3.3×/60	50	20	40
L176F	390	(250)/3.7×/60	60	70	120
I177M	20	(20)/1.4×/20	4	2	10
G182C	260	(170)/3.8×/70	60	10	30
T189I	430	(60)/0.9×/—	40	0	0
V192F	230	(50)/1.2×/20	20	0	0
L216F	350	(220)/3.7×/60	70	0	0
G240V	80	(170)/12×/210	30	2	100
L453F	190	(40)/1.4×/20	50	0	0
E476Q	40	(30)/3.6×/90	3	50	70
N483S	115	(140)/6.8×/120	70	0	0
T189I/G680V	90	(200)/13×/220	5	10	30
L453F/G680V	30	(70)/13×/220	5	70	130
L176F/L453F	550	(80)/0.9×/—	20		

[a] Basal (Mg^{2+}-ATP), actin-enhanced (Mg^{2+}-ATP and 1 mg/ml actin), and Ca^{2+}/salt (Ca-ATP + 600 mm KCl) ATPases relative to wild type (100%) are shown. Data are shown to the nearest 10%. For ATPase enhancement by 1 mg/ml actin, the data are presented as percentage of wild-type ATPase with 1 mg/ml actin/fold increase of ATPase rate by 1 mg/ml actin (compared to mutant's basal ATPase)/percentage of wild-type ATPase acceleration. Basal ATPase for wild type was ~2.5 nmol P_i liberated per nanomole of myosin per minute.

[b] Performance of cytoskeletal ghosts prepared from Dictyostelium cells expressing mutant or wild-type myosin are indicated. Contraction events were observed by recording ATP-induced, contraction-derived changes in light scattering of ghosts in a stopped-flow chamber.

[c] Comparison of the calculated initial velocity of change in light scattering after addition of ATP.

[d] Comparison of the total change in light scattering after addition of ATP.

isolated in the region between amino acids 125 and 240 (P128Q, L175F, L176F, I177M, G182C, T189I, V192F, L216F, and G240V), as well as those between amino acids 450 and 500 (L453F, E476Q, and N483S; Figure 1). We also included two double mutants (representing the suppressed state of the motor), T189I + G680V and L453F + G680V, as well as one double mutant containing two of the suppressor mutations in the absence of G680V, L176F + L453F.

ATPases: The basal ATPase rate of most of the mutants was enhanced two- to fourfold compared to that of the wild type (Table 1). This is a satisfying contrast to the behavior of the G680V mutant, to which the suppressors restore function. However, this trait was not a universal characteristic of the suppressors. S1.P128Q, S1.I177M, S1.G240V, S1.E476Q, and S1.N483S all exhibited depressed or near-normal basal ATPase rates. There are three possible explanations for this difference in behavior: (1) the ATPase nonenhancing mutants are acting through a different mechanism than the others, (2) the behavior of suppressors in isolation does not reflect their effect when combined with the G680V mutation, or (3) the mutant does not fare well in the purification or under the assay conditions. The double mutants with G680V displayed activities intermediate between the two single mutations they combined. The L176F + L453F double mutant S1 showed the greatest level of basal ATPase that we observed, fivefold that of wild type.

The enhancement of ATPase effected by the addition of 1 mg/ml filamentous actin ("actin enhancement") was also measured (Table 1). In wild type, actin accelerates the ATPase by enhancing rates of P_i release. None of the mutants with enhanced basal ATPase rates displayed the same degree of enhancement upon addition of actin as the wild type [as assessed by calculating (1 mg/ml actin-enhanced ATPase)/(basal ATPase)]. Some nonetheless exhibited significant increases (S1.L175F, S1.L176F, S1.G182C, and S1.L216F), while others displayed essentially no increase (S1.T189I, S1.V192F, and S1.L453F). Of the mutants that did not show elevated basal ATPase, only I177M failed to show near-normal or better enhancement upon addition of 1 mg/ml actin.

Actin release: One of the key events that must be coordinated for motor function is the coupling of actin binding and release to the presence, absence, or state of nucleotide. To assess the mutants' ability to respond appropriately to nucleotide, we measured the propor-

TABLE 2

Percentage of S1 not bound to actin

Mutant	Rigor	Rigor/KCl	1 mm ATP	ATP/KCl	5 mm ADP	ADP/KCl	1 mm ATPγS
Wild type	10	10	80	100	20	50	60
G680V	20	30	30	80	10	20	80
P128Q	30	30	80	80	50	60	30
L175F	10	10	90	100	50	60	70
L176F	0	0	90	90	0	20	80
I177M	0	10	90	100	60	80	80
G182C	0	10	80	90	40	60	70
T189I	0	10	30	50	0	0	0
V192F	0	0	90	90	10	10	20
L216F	10	10	70	80	10	10	20
G240F	0	0	60	70	10	20	10
L453F	10	10	70	80	10	20	20
E476Q	20	70	80	90	50	100	80
N483S	20	10	80	90	30	60	70
T189I/G680V	20	40	80	100	20	30	90
L453F/G680V	20	30	90	100	20	40	90

Actin-binding/nonbinding properties of mutants at 20°. Since the effect of the added nucleotide is to prevent binding to actin, we have represented the data as percentages of S1 remaining in the supernatant after spinning. The first column indicates the S1 sequence, and other columns indicate salt (0 or 250 mm KCl) and nucleotide additions (1 mm ATP, 5 mm ADP, or 1 mm ATPγS) made to each sample (rigor indicates no nucleotide added). Thus, comparisons with the rigor column yield the additional quantity of S1 liberated from actin by nucleotide or salt addition.

tion of S1 coprecipitated with actin filaments in the absence of nucleotide and in the presence of 5 mm ADP, 1 mm ATP, or 1 mm ATPγS (Table 1). Since we have previously characterized a unique salt sensitivity of actin binding of S1.G680V in the presence of 250 mm KCl, we also performed the no-nucleotide, ADP, and ATP coprecipitations in the presence of this salt. We have reported the data in terms of actin release (or nonbinding) since it is this effect of salt or nucleotide addition that we are determining. Release is quantified as (Total input myosin) − (myosin in pellet after spinning).

In the absence of nucleotide, all mutants exhibit wild-type-like behavior. The addition of salt has dramatic effects on only one mutant, S1.E476Q, which is largely released from actin by this treatment. In the presence of ATP, all mutants behave similarly to the wild type, except for only S1.T189I, which shows significant cosedimentation both in the presence and absence of KCl.

The presence of other different, relevant forms of nucleotide has differential effects on the mutants (Table 2). While several mutants exhibit release within the normal range effected by 5 mm ADP (0–20% release), five show substantially increased release (S1.P128Q, S1.L175F, S1.I177M, S1.G182C, and S1.E476Q). A wholly different set fails to reflect the wild type's enhanced release upon addition of both ADP and 250 mm KCl—S1.T189I, S1.V192F, S1.L216F, S1.G240V, and S1.L453F. These same mutants, barring only S1.L176F, also fail to demonstrate significant release in the presence of even 1 mm ATPγS. While the mutants are soluble in the presence of ATPγS, we cannot rule out that the addition of actin results in aggregation.

Cytoskeletal contractility: We measured both the initial rate of contraction (actually the initial rate of change in light scattering) and the extent of change in contraction (light scattering) achieved by tritonized cytoskeletal ghosts (containing full-length myosins) upon addition of ATP. We interpret the initial rate as a reflection of a minimally loaded contraction, while the extent seems most likely to be a reflection of the ability of the mutant filaments to exert and hold force. For example, in the contractility assay, the G680V mutant shows very slow initial rates of contraction, but eventually achieves ~60% of the contraction extent of the wild type (Table 1). This is consistent with its behavior in the "classical" motility assay, in which fluorescent actin filaments are translocated by anchored myosin heads or filaments. In this assay, G680V myosin drives slow movement on its own and interferes with wild-type motility in mixing experiments (Patterson *et al.* 1997).

The ability of the different mutants to achieve cytoskeletal contraction correlated with their *in vivo* phenotype. The mutants that failed to exhibit contraction in the assay (P128Q, T189I, V192F, L216F, L453F, and N483S) included all those that showed myosin-null cell rates of plaque expansion on bacterial lawns (Patterson 1998). Only the P128Q mutant lacked contraction *in vitro* while showing better than myosin-null cell rates in terms of plaque expansion on bacterial lawns.

Conversely, the G680V mutant showed significant evidence of cytoskeletal contraction *in vitro*, but it did not improve myosin-null cell rates in terms of plaque expansion. The rate and extent of contraction did not always exhibit a one-to-one correspondence, as would be expected if the values represent force production (maximizing for number of heads actively stroking) and unloaded contraction rate (maximizing release rates). The most dramatic example is the G240V mutant, which shows only 2% of the wild-type contraction rate, but eventually achieves the same extent of contraction as the wild type.

DISCUSSION

We have proposed that the G680V mutation of Dictyostelium myosin II introduces an interruption of the smooth functioning of the myosin motor cycle after initial productive contact with actin (Patterson *et al.* 1997). This deduction is based on the braking behavior of G680V mutants on their wild-type counterparts in mixing experiments and on the unique salt sensitivity of a prolonged actin-interacting state observed in the presence of ATP. In wild-type myosin motors, actin acts catalytically to enhance the ATPase by greatly accelerating the rate of P_i release; in the G680V mutant, we suggest that the energetic barrier to P_i release is higher, rendering turnover rates lower in the presence and absence of actin. We reasoned that intragenic suppressors of the G680V mutation would represent compensatory derangements of the myosin cycle. If the flaw blocking the biological function of the G680V mutant myosin lies in the prohibitive barrier to P_i release, then a common mechanism of suppression should facilitate this event. Since the basal ATPase rate is limited by P_i release, a common property of suppressor mutations should be enhanced rates of basal ATPase. Mutations conferring this phenotype will provide insight into the mechanisms of P_i restriction and release.

Rationale: We had three goals in characterizing the myosin motors bearing suppressor mutations: (1) to determine the spectrum of changes (relative to wild type) that could compensate for the G680V mutation, (2) to identify common properties of suppressor mutations to gain insight into structural/mechanical aspects of motor function, and (3) to test the model proposing that the G680V mutation specifically impairs P_i release by the motor by observing the types of changes required to restore a motor bearing this mutation to function. We have focused on the effects of suppressor mutations in the absence of G680V, as the phenotypes of the revertants indicate that the properties of the G680V mutation and its suppressor in combination biologically cancel each other out. In our analysis, we focus on the differences in properties of the mutants *vs.* wild type. In this way, we determine the functional alterations required to repair an "unbalanced" motor. By looking at a large number of suppressors and their characteristics, we extract themes common to the group. The most notable of these, enhanced basal ATPase, reflects precisely the property one would predict to be required to restore function to a mutant with impaired P_i release.

Common altered properties of suppressor mutants: One striking feature of our results is the behavioral similarities of the G680V suppressor mutants. The suppressors we report in this study were previously noted for their three-dimensional clustering and common property of increasing amino acid residue volume. These same mutations have common differences from the wild type in terms of elevated basal ATPase, limited or absent ATPase enhancement by 1 mg/ml actin, and failure to exhibit ADP- or ATPγS-stimulated release from actin. Despite the clear biochemical unification, individual mutants may not subscribe to one or more of the group features. These relationships are summarized in the Venn diagram in Figure 2. Nearly all suppressors show enhanced basal ATPase, suggesting that this feature lies at the heart of the suppression mechanism. Most also show aberrant responses to ATPγS and ADP (in the presence of KCl), suggesting that these features are intimately related to alterations in basal ATPase.

While this set of properties joins the bulk of the mu-

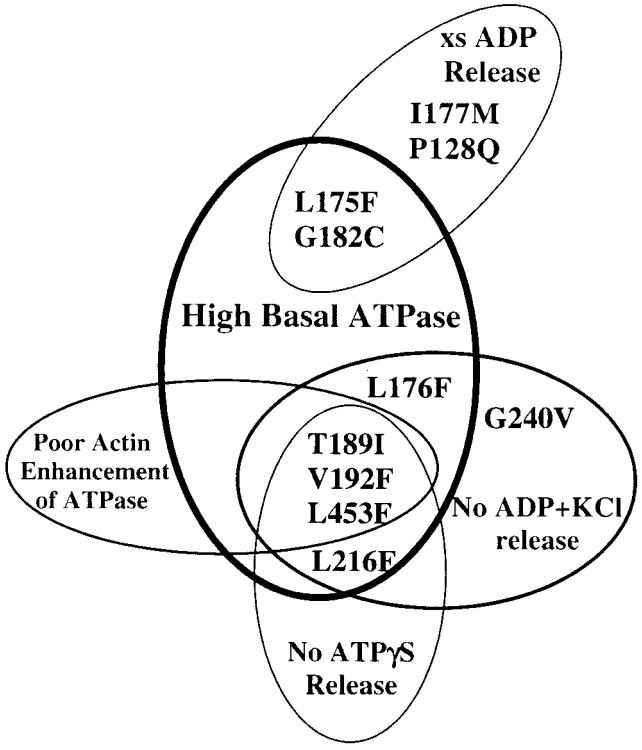

Figure 2.—Venn diagram of suppressor properties. Mutants sharing similar deviations from wild-type behavior are joined within ellipses. The property indicated by a given ellipse is written within the ellipse in outline font. Properties are discussed within the text. E476Q and N483S mutants are not shown since they do not fit into this schema.

tants in a general way, they can also be subdivided. For example, while S1.G182C and S1.T189I both exhibit elevated basal ATPase, they differ strikingly in their nucleotide-induced release from actin. While the wild type shows roughly equal amounts of release with and without ADP, S1.G182C goes from no S1 released to ~40% released upon the addition of ADP; further addition of KCl or addition of ATPγS results in an almost quantitative release. S1.T189I, on the other hand, exhibits normal release (or lack thereof) by ADP, but it is resistant to release induced by KCl + ADP and ATPγS. We take these similarities and differences to be indicative of meaningful differences between similarly timed states of the myosin motor. In general, while the majority of the mutations facilitate P_i release, some have consequences for nucleotide affinity while others have an ancillary effect on the conformational state of the motor bound to ADP. We discuss the varying motor defects induced by the suppressor mutations on a property-by-property basis below.

Elevated basal ATPase: The strongest and most easily testable of our predictions of G680V suppressors is that they should include mutations that facilitate P_i release. Since P_i release is the rate-limiting step in the basal (actin-independent) ATPase of myosin, acceleration of this step in the mutants is easily detected. Of the 13 mutants tested, 7 dramatically elevate this activity (as summarized in Figure 3). These are the motors bearing the L175F, L176F, G182C, T189I, V192F, L216F, and L453F mutations. Strikingly, this group includes five of the six mutations we termed "the cluster" on the basis of their three-dimensional grouping in the myosin structure. I177M does not show enhanced basal ATPase and happens to be the only member of the cluster that did not undergo a significant increase in volume. G182C and L216F were not included in the original group because spatially they are "satellites" of the cluster, but the similarities between their properties and those of the cluster are sufficiently striking to suggest that they influence myosin conformational preferences in a similar manner. Thus, our designation of the cluster as a set of mutations with common spatial and chemical properties is reinforced by the mutants' biochemical properties. The finding that a double mutant made from two members (L176F + L453F) has a basal ATPase exceeding that of either mutant alone (and the highest value we have observed) argues that basal ATPase elevation is occurring via common or compatible mechanisms in at least these two cases. Our ability to endow myosin with still more exaggerated properties by introducing combinations of similarly behaving mutations suggests that these mutants may be useful for driving conformational changes in the motor that will be independent of normal inducers (such as actin filaments). We anticipate that some combination of these mutations will allow crystallographic observations of heretofore inaccessible states, *i.e.*, those involved in P_i release.

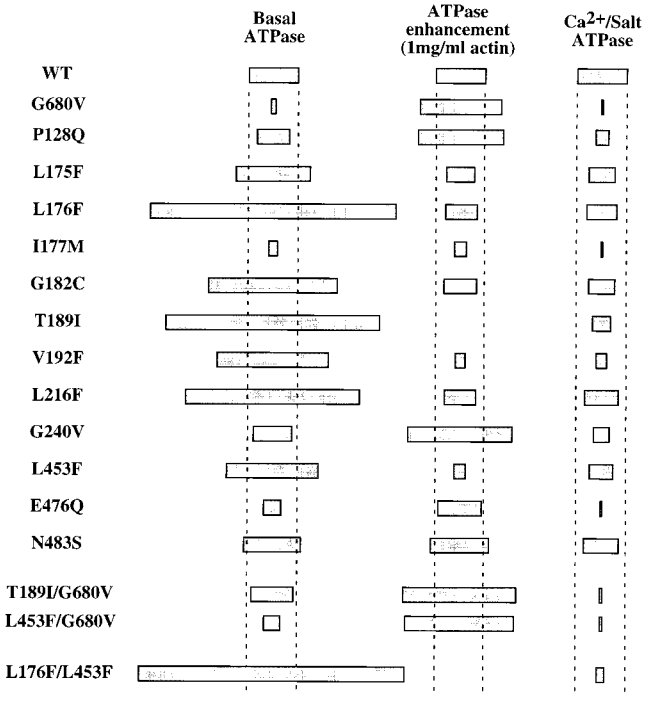

Figure 3.—ATPase properties of G680V and suppressors. ATPase activities of mutants are shown relative to wild type. Wild-type activity is arbitrarily designated 100% and marked by dashed lines. The relative activity of each mutant is indicated by the width of the bar. Basal refers to Mg^{2+}-ATPase in the absence of actin, ATPase enhancement refers to Mg^{2+}-ATPase in the presence of 1 mg/ml actin, and Ca^{2+}/Salt ATPase refers to Ca^{2+}-ATPase in the presence of 600 mm KCl.

Lack of ATPase acceleration induced by 1 mg/ml actin: A key property of a properly tuned myosin motor is the enhancement of ATPase activity observed in the presence of actin. Given that many of the mutations accelerate the basal ATPase (thus reflecting a lowered energetic barrier to P_i egress), we were curious to see whether actin would continue to exert its accelerating effect. Under the standard conditions, we used 1 mg/ml actin, and many of the mutant motors showed little, if any, increased ATPase activity compared to the absence of actin, while a minority displayed a degree of enhancement proportional to that of the wild type. Of the mutants exhibiting enhanced basal ATPase, some showed little or no enhancement of ATPase activity by 1 mg/ml actin (T189I, V192F, and L453F), while the others showed significant enhancement, but still less than that of the wild type (L175F, L176F, G182C, and L216F). It is interesting to note that two of the mutants with the highest rates of basal ATPase (L176F and L216F) nonetheless showed significant enhancement by 1 mg/ml actin, demonstrating that raising the basal ATPase does not cause an obligate loss of further acceleration by actin. This would be consistent with a mechanism in which the suppressor mutation lowers the energetic barrier to P_i release, but does not abolish it, and actin acts in a nonredundant fashion to further enhance release.

Changes in actin release: In the absence of nucleotide (rigor binding conditions), almost all mutants responded in a manner similar to the wild type, including the G680V mutant itself. The singular exception is the E476Q mutant, which as an S1 displays dramatic salt sensitivity of rigor binding. The majority of S1.E476Q remained in the supernatant in the presence of 250 mm KCl. This finding is consistent with the results of Friedman *et al.* (1998), who concluded that the similar S1.E476K mutant myosin was unable to enter strongly bound states. Since the E476Q mutation is unique among G680V suppressors in this property, we conclude that it represents a different "solution" to the G680V-induced defects of the motor. It is not clear whether its sharing the property of enhanced release from actin in the presence of 5 mm ADP with other suppressors is a result of conformational similarity with these other mutants (P128Q, L175F, I177M, and G182C) or a reflection of its general strong binding failures. It should be noted that despite its failings *in vitro*, full-length E476Q myosin behaves essentially as the wild type in our plaque expansion (SPERA) assay, indicating that it is able to provide at least one form of myosin function *in vivo*. Similarly, in our contractility assay, it performs at 50% of the wild type's initial rate and achieves 70% of the wild type's final contraction.

Other than T189I, which exhibits significant retention of actin binding in the presence of ATP both with and without salt, all mutants are essentially normal for ATP-induced release from actin. In the presence of ADP and ATPγS, the mutants can be divided into two groups—those that show enhanced release in the presence of ADP (P128Q , L175F, I177M, and G182C) and those that show little or no release in the presence of 1 mM ATPγS (T189I, V192F, L216F, G240V, and L453F). In combination, these two groups include all the suppressors with elevated basal ATPase (as well as others), except for only L176F, suggesting that they embody mutually exclusive facets of basal ATPase enhancement. Mutants that fail to respond to ATPγS are particularly intriguing given their apparently normal response to ATP: wild-type release from actin induced by 10 μm ATPγS exceeds that of the ATPγS-insensitive mutants at 1 mm, but release of the same mutants at 1 mm ATP is essentially normal. This is another example of a phenotype complementary to that of the G680V starting mutant, which is ~100-fold *more* sensitive to ATPγS-induced actin release than the wild type (Patterson *et al.* 1997).

Double mutants: To demonstrate that the suppressors were indeed acting to reverse or ameliorate the key *in vitro* defects of the G680V mutation, we characterized two double mutants, T189I + G680V and L453F + G680V. *In vivo*, both double mutants show near-wild-type behavior, whereas all three single mutants are indistinguishable from myosin null in the SPERA assay. As anticipated, these double mutants showed behaviors more akin to wild type than either mutant parent, at least in cases where the mutant deviated significantly from wild-type behavior. The only significant shortcomings compared to wild type behavior are the following: (1) both double mutants show lower basal ATPase than wild type, though they are intermediate between their two parental mutants; (2) both show greater actin enhancement of basal ATPase than wild type under our standard conditions; and (3) both continue to display depressed Ca^{2+} ATPase activities, suggesting that this activity, while severely impaired in the G680V mutant, is not innately reflective of a critical defect for *in vivo* function.

Groups of mutants and states of the motor: Our most striking finding is the overlap in properties between the G680V suppressors characterized in this study. As shown in Figure 2, almost all the suppressors share common features, with many mutants exhibiting several. T189I, V192F, and L453F mutations confer a core set of properties that overlap to some extent with all the other suppressors, except for E476Q and N483S. These properties include high basal ATPase and poor actin enhancement of ATPase. These are logical properties if these suppressors act by counteracting the conformational imbalance(s) introduced by the G680V mutation. As we have suggested previously (Patterson *et al.* 1997), one reasonable scenario for the action of the G680V mutation and its suppressors is by influencing the open/closed state of the "backdoor" route of P_i release, as hypothesized by Yount *et al.* (1995). The backdoor route is blocked by residues R238 and E459 in the Dictyostelium vanadate structure, but it is partially accessible in the beryllium fluoride structure. This difference lends support to the model of Yount *et al.* (1995) and sketches the conformational changes that may be involved. The backdoor's change of state is mediated by a rotation of the "camshaft" helix (residues 466–496, red in Figure 1), which brings residue E459 with it. Note that two mutations (E476Q and N483S) alter residues within this helix, while the rest cluster above and to one side of it, notably those in the 175–195 range and L453F. The G240 position could well directly influence the disposition of R238. As we noted, the G680V mutation increases bulk on one side of the helix toward its C terminus and would plausibly raise the energetic requirement for a counter-rotation required to open the backdoor. On the other hand, the suppressors increase bulk on a region of the helix toward its center, but they also rotate 120° relative to the G680V mutation and, thus, could act to counter it, presumably facilitating rotation toward the "backdoor open" position. Our finding that G680V suppressors raise the basal ATPase (for which P_i release is the rate-limiting step) is wholly consistent with this view. The origin of several of the phenotypes shared by many of the suppressors (failure to release actin in the presence of ATPγS, failure to release actin in the presence of ADP and KCl) are not intuitively obvious. We submit

that these are ancillary effects of conformational alterations that bring about enhanced P_i release.

Two of the mutants studied, E476Q and N483S, do not fit into our neat summary. It should first be noted that their location and structural changes marked them as different from the start. Both are on the same side of the camshaft (helix 466–496) as the G680V mutation, both are hydrophilic residues (most of the other suppressors mutate hydrophobic residues, particularly leucines), and neither mutation represents an increase in volume (indeed, out of the 19 suppressors identified, only N483S resulted in the substitution of a significantly smaller residue). N483S may be the particular case of a suppressor that acts by directly reversing the effect of the primary mutation: it is positioned to create room for the increase in bulk introduced by the G680V change. The E476Q mutation is more intriguing. E476 faces the region of the structure thought to represent the primary actin-binding interface. It has a lowered basal ATPase and is dramatically impaired in rigor (ATP-free) binding to actin in the presence of 250 mm KCl. The more severely affected E476K mutant is reported to be unable to enter the strongly bound state of actin interaction (Friedman *et al.* 1998). The route by which the E476K mutation suppresses the G680V change is unclear. Given our interpretation of the G680V mutation, we might have hypothesized that a suppressor would act by increasing the likelihood of a transition to a strong binding state (since this transition is closely correlated with P_i release), but this is apparently not the case. One uninteresting possibility is that the mutation acts indirectly; by weakening the strongly bound state, it could alleviate the "braking" effect of paused/arrested myosins, allowing those motors that reached the stroking phase to proceed unimpeded.

Use of suppressor mutations to enlighten structure/function studies: Our findings demonstrate several ways by which a suppressor approach can inform the dissection of the function of a biomolecule. First, the suppressor mutations by definition reverse the critical defect(s) of the starting mutant. It is therefore reasonable to anticipate that suppressor properties in isolation will be complementary to the primary mutation in some regard. In the case of the G680V mutation, this is particularly propitious in that the proposed defect of the mutant, impaired release of P_i after ATP hydrolysis, is particularly difficult to demonstrate. In contrast, the complement of reluctant P_i release, promiscuous release of P_i, is readily observed as a heightened basal ATPase. An added benefit is that the suppressors can confirm or deny that a property observed *in vitro* is the critical one *in vivo*—the majority of the mutations indeed enhance P_i release, whereas none of them restore the debilitated Ca^{2+} ATPase, indicating that the latter does not reflect a critical property *in vitro*.

Suppressor alleles can also illuminate structural components and interactions in the biomolecule under study. In general, it will be easy to select suppressors in that they will often be defined as alterations that restore wild-type function. Thus, a number of them can be recovered and by their very number will provide powerful constraints on models of function. In this case, the existence of several mutants with overlapping properties (see Figure 3) that are also spatially and chemically restricted has allowed us to promulgate a specific hypothesis of motor function, to wit, that the disposition of the camshaft (helix 466–496) determines the open or shut state of the backdoor (residues R238 and E459). A single mutation or suppressor could represent an arbitrary solution, or its key property might be difficult to deduce. Finally, suppressors that confer biochemical phenotypes provide tools for direct understanding of function, while those that produce biological phenotypes on their own represent tools for further genetic manipulation (Jarvik and Botstein 1975).

Details of ongoing work can be found at http://research.biology.arizona.edu/myosin.

We gratefully acknowledge Taro Uyeda and Roy Parker for enlightening discussions and Therence DeCorse and Meghan Kreeger for media creation. Figure 1 was generated using SPdbViewer and POV-Ray software. This work was supported by National Institutes of Health grant GM55977, American Heart Association Arizona Affiliate grant AZBG-19-95, and an Arizona Institutional Small Grant.

LITERATURE CITED

Aguado-Velasco, C., and E. R. Kuczmarski, 1993 Contraction of reconstituted *Dictyostelium* cytoskeletons: an apparent role for higher order associations among myosin filaments. Cell Motil. Cytoskelet. **26:** 103–114.

Friedman, A. L., M. A. Geeves, D. J. Manstein and J. A. Spudich, 1998 Kinetic characterization of myosin head fragments with long-lived myosin·ATP states. Biochemistry **37:** 9679–9687.

Giese, K., and J. A. Spudich, 1997 Phenotypically selected mutations in myosin's actin binding domain demonstrate intermolecular contacts important for motor function. Biochemistry **36:** 8465–8473.

Jarvik, J., and D. Botstein, 1975 Conditional-lethal mutations that suppress genetic defects in morphogenesis by altering structural proteins. Proc. Natl. Acad. Sci. USA **72:** 2738–2742.

Kuczmarski, E. R., L. Palivos, C. Aguado and Z. Yao, 1991 Stopped-flow measurement of cytoskeletal contraction: *Dictyostelium* myosin II is specifically required for contraction of amoeba cytoskeletons. J. Cell Biol. **114:** 1191–1199.

Manstein, D. J., and D. M. Hunt, 1995 Overexpression of myosin motor domains in *Dictyostelium*: screening of transformants and purification of the affinity tagged protein. J. Muscle Res. Cell Motil. **16:** 325.

Patterson, B., 1998 Intragenic suppressors of Dictyostelium myosin G680 mutants demarcate discrete structural elements: implications for conformational states of the motor. Genetics **149:** 1799–1807.

Patterson, B., K. M. Ruppel, Y. Wu and J. A. Spudich, 1997 Cold-sensitive mutants G680V and G691C of Dictyostelium myosin II confer dramatically different biochemical defects. J. Biol. Chem. **272:** 27612–27617.

Smith, C. A., and I. Rayment, 1996 X-ray structure of the magnesium(II)·ADP·vanadate complex of the *Dictyostelium discoideum* myosin motor domain to 1.9Å resolution. Biochemistry **35:** 5404–5417.

Spudich, J. A., and S. Watt, 1971 The regulation of rabbit skeletal muscle contraction. I. Biochemical studies of the interaction of

the tropomyosin-troponin complex with actin and the proteolytic fragments of myosin. J. Biol. Chem. **246:** 4866–4871.

Sussman, M., 1987 Cultivation and synchronous morphogenesis of *Dictyostelium* under controlled experimental conditions, pp. 9–29 in *Dictyostelium discoideum: Molecular Approaches to Cell Biology*, edited by J. A. Spudich. Academic Press, Orlando, FL.

White, H. D., 1982 Special instrumentation and techniques for kinetic studies of contractile systems, pp. 698–708 in *Structural and Contractile Proteins, Part B. The Contractile Apparatus and the Cytoskeleton*, edited by D. W. Frederiksen and L. W. Cunningham. Academic Press, New York.

Yount, R. G., D. Lawson, and I. Rayment, 1995 Is myosin a "back door" enzyme? Biophys. J. **68:** 44s–49s.

Communicating editor: A. G. Hinnebusch